

Laboratory Investigation into the Effects of Silty Fines on Liquefaction Susceptibility of Chlef (Algeria) Sandy Soils

Hanifi Missoum · Mostefa Belkhatir ·
Karim Bendani · Mustapha Maliki

Received: 21 February 2011 / Accepted: 1 November 2012 / Published online: 13 November 2012
© Springer Science+Business Media Dordrecht 2012

Abstract In a number of recent case studies, the liquefaction of silty sands has been reported. To investigate the undrained shear and deformation behaviour of Chlef sand–silt mixtures, a series of monotonic and stress-controlled cyclic triaxial tests were conducted on sand encountered at the site. The aim of this laboratory investigation is to study the influence of silt contents, expressed by means of the equivalent void ratio on undrained residual shear strength of loose, medium dense and dense sand–silt mixtures under monotonic loading and liquefaction potential under cyclic loading. After an earthquake event, the prediction of the post-liquefaction strength is becoming a challenging task in order to ensure the stability of different types of earth structures. Thus, the choice of the appropriate undrained residual shear strength of silty sandy soils that are prone to liquefaction to be used in engineering practice design should be established. To achieve this, a series of undrained triaxial tests were conducted on reconstituted saturated silty sand samples with different fines contents ranging from 0 to 40 %. In all tests, the confining pressure was held constant at

100 kPa. From the experimental results obtained, it is clear that the global void ratio cannot be used as a state parameter and may not characterize the actual behaviour of the soil as well. The equivalent void ratio expressing the fine particles participation in soil strength is then introduced. A linear relationship between the undrained shear residual shear strength and the equivalent void ratio has been obtained for the studied range of the fines contents. Cyclic test results confirm that the increase in the equivalent void ratio and the fines content accelerates the liquefaction phenomenon for the studied stress ratio and the liquefaction resistance decreases with the increase in either the equivalent void ratio or the loading amplitude level. These cyclic tests results confirm the obtained monotonic tests results.

Keywords Silt · Sand · Liquefaction · Shear strength · Void ratio

List of symbols

CLR	Cyclic liquefaction resistance
CSR	Cyclic stress ratio
C_u	Coefficient of uniformity
D_r	Initial relative density
e	Global void ratio
e_{\max}	Maximum void ratio
e_{\min}	Minimum void ratio
e_s	Inter-granular void ratio
e^*	Equivalent void ratio
F_c	Fines content

H. Missoum (✉) · K. Bendani · M. Maliki
Laboratory of Construction, Transports and Environment
Protection (LCTPE), University of Mostaganem,
Mostaganem, Algeria
e-mail: hanifmissoum@yahoo.fr

M. Belkhatir
Laboratory of Materials Sciences and Environment,
University of Chlef, Chlef, Algeria

G_s	Specific gravity of soil grain
N_c	Number of cycles
p'	Effective mean stress
p'_s	Effective mean stress at steady state
q	Deviatoric stress
q_m	Loading amplitude
q_s	Deviatoric stress at steady state
S_{us}	Undrained residual shear strength
ε_a	Axial strain
ϕ_s	Mobilized angle of inter-particle friction at steady state
γ_d	Solid dry density
σ_c	Confining pressure

1 Introduction

The city of Chlef is located in the near field of the ruptured fault. On 10 October 1980, the area of Chlef experienced a substantial damage during the earthquake event. This natural disaster affected dramatically the city and the neighbouring areas. Consequently, many buildings and infrastructures were either collapsed or partially demolished.

A quite remarkable observation from the geotechnical point of view was the occurrence of numerous cases of ejection onto the ground surface level of great masses of sandy soils and large displacements of various forms of some equipment foundations.

Based on the post-earthquake observations, it is essential to assess the factors that might contribute to these damages, which are due partly to soil liquefaction problem during seismic shaking.

Recent case studies reported that significant damages to embankments, earth dams, building foundations, and infrastructure can be produced by liquefaction generated by a cyclic motion. The greatest impact could be seen at destroyed infrastructure, especially bridge supports, container ports and landslides. Undrained saturated sandy soils could lose part of their strength during these natural events. This is caused by an excess pore pressure and, therefore, a fall in the normal effective stress, resulting in a decrease in the strength of the soil skeleton. The factors that may affect the liquefaction of clean sand are broadly investigated (Idriss and Boulanger 2008). However, the understanding of liquefaction phenomenon of sand–silt mixtures is not complete and needs more study.

Most of the previous researches on liquefaction were conducted on clean sands with the assumption that the behaviour of silty sand is similar to that of clean sands. Recently, researches by Zlatovic and Ishihara (1995), Lade and Yamamuro (1997), Thevanayagam (1998), Naeini and Baziar (2004) and Maheshwari and Patel (2010) have shown that in some cases, sand deposited with silt content is much more susceptible to liquefaction than clean sand. Moreover, deformation characteristics and pore pressure development in silty sand samples are quite different from clean sand. These conclusions emphasize the importance of deposits with mixture of sand and silt. At present time, the behaviour of silty sand soils is still not clearly known during earthquake.

Further, the post-earthquake behaviour of silty sand and, consequently, the stability of structures founded on liquefied soil depend on the post-liquefaction shear strength of soil. The strength of soils at the phase transition or at the quasi-steady state has an important implication for engineering practice (Ishihara 1993). In the last 10 years, laboratory studies have contributed much to clarify the main parameters that affect the residual shear strength and provide some principles for selecting it for design.

Meanwhile, the selection of suitable undrained residual shear strength for design and analysis is still under investigation and needs a broad consensus (Finn 2000).

Soil mixtures such as silty clays, clayey sands and silty sands are more commonly found in nature and in earth structures than pure sands, silts and clays. However, the behaviour of soil mixtures is not well understood since soil mechanics has concentrated mostly on pure soils. This is particularly true for soils containing non-plastic silty fines. Most of the recent studies have pointed out that the liquefaction potential depends on the fines content fraction, and the trend is essentially related to the quantity of fines hosted by the sand.

Results from many laboratory investigations are controversial. This is especially valid for soils containing non-plastic silty fines. The engineering stress–deformation characteristics of the soil structure depend on its nature, and the soil behaves as a collection of scale-level-dependent skeletons arranged in a particular manner (Thevanayagam 1997; Thevanayagam and Nesarajah 1998); as a result, the physical nature of silty sand should be entirely

different from clean sand (Thevanayagam 1998; Yamamuro and Lade 1998; Naeini and Baziar 2004). In all these studies, it is recognized that the undrained residual shear strength response depends effectively on the void ratio and the fines content. Moreover, several studies have reported that increasing the fines content in a sand will improve the liquefaction resistance of the sand (Singh 1994; Carraro et al. 2003), decrease the liquefaction resistance of the sand (Troncosco and Verdugo 1985; Georginnou et al. 1990; Zlatovic and Ishihara 1997) or decrease the liquefaction resistance until a certain value of fines content is reached, and then increase its resistance (Law and Ling 1992; Koester 1994; Bouferra and Shahrouf 2004). Thus, numerous studies have reported that the behaviour of sand hosting fine-grained soils depends mainly on the gradation of host sand, the fines content and their plasticity index. Indeed, to a certain value of fines content, fractions of fine-grained soils occupy solely the voids and do not affect the behaviour of the mixture. For this reason, the notion of skeleton void ratio was suggested to characterize those kinds of soils (Kenny 1977; Mitchell 1993).

Therefore, it is quite important to introduce new index parameters such as the equivalent void ratio (Thevanayagam et al. 2002) to predict the undrained residual shear strength response of sand–silt mixtures as well as to express mechanical behaviour by means of non-plastic fines content.

The cyclic stress approach (Seed and Idriss 1981) and the cyclic strain approach (Dobry et al. 1982) are commonly used in order to evaluate the liquefaction potential of sands; meanwhile, fine-grained soils such as silts, clayey silts and sands with fines were considered non-liquefiable. However, recent case studies of earthquakes have revealed liquefaction of many cohesive soils during earthquake. These cohesive soils had clay fraction less than 20 %, liquid limit between 21 and 35 %, plasticity index between 4 and 14 %, and water content more than 90 % of their liquid limit. Kishida (1969) reported liquefaction of soils with up to 70 % fines and 10 % clay fraction during Mino-Owari, Tonankai and Fukui earthquakes. Seed et al. (1983) found that some soils with fines may be highly susceptible to liquefaction.

Therefore, based upon conflicting results presented in the literature, the fines content of a sandy soil does not provide a definitive behavioural trend, and despite the great progress in physical modelling of

liquefaction, a number of challenges still remain. In this contribution, our main concern is focused on introducing a unified treatment of Chlef silty sand behaviour at different relative densities.

In order to achieve this aim, a series of monotonic and cyclic undrained triaxial tests were conducted on reconstituted saturated silty sand samples with different fines contents.

2 Materials and Methods

2.1 Materials Under Investigation

Chlef sand has been used in this experimental research programme. Sand samples were collected from liquefied layer of the deposit areas of the region. The predominant minerals of the current sand are feldspar and quartz. Individual sand particles are rounded. The tests were performed on the mixtures of Chlef sand and silt. Liquid limit and plastic limit of the silts were 27 and 22 %, respectively. Since liquefaction susceptibility of a soil is mainly controlled by its relative density (Yamamuro and Kelly 2001) and because Chang et al. (1982) have revealed that most liquefactions resulting from earthquakes have occurred in silty sands and sandy silts, different silt contents ranging from 10 to 40 % were mixed to Chlef sand during this work. Previous experimental research studies on methods of deposition have revealed that the mechanical behaviour of sandy soils depends mainly on the mode of the sample preparation (Della et al. 2009). The sample must be prepared in such a way to replicate the soil conditions at the field. There are several methods used to prepare soil sample in the laboratory such as moist tamping, dry pluviation and water sedimentation. Among them, Vaid et al. (1999) have shown that dry pluviation specimens tend to reproduce well field performance of sands. Dry pluviated samples tend to show dilative behaviour even when prepared in their loosest state (Vaid et al. 1999). In this present study, the soil samples are prepared by the dry pluviation method for the monotonic and cyclic loading. However, experimental data related to the effect of depositional methods on the behaviour of sand with low plastic fines are very limited because most of the previous studies have concentrated their efforts on clean sand (Yamamuro and Wood 2004). The geotechnical properties of the soils used during this study are summarized in Table 1.

Table 1 Geotechnical properties of Chlef sand–silt mixtures

Material	F_c Fines content (%)	G_s Specific gravity of soil grain	D_{50} (mm)	D_{10} (mm)	C_u	e_{min}	e_{max}
Clean sand	0	2.680	0.68	0.158	2.90	0.535	0.854
Silty sand	10	2.682	0.50	0.079	7.75	0.472	0.798
Silty sand	20	2.684	0.43	0.038	15.26	0.431	0.748
Silty sand	30	2.686	0.37	0.022	23.18	0.412	0.718
Silty sand	40	2.688	0.29	0.015	27.33	0.478	0.732
Silty sand	50	2.69	0.08	0.011	28.18	0.600	0.874
Silt	100	2.70	0.057	0.003	34.16	0.72	1.420

The grain size distribution curves for the soils are illustrated in Fig. 1. D_{50} and D_{10} correspond to the soil diameters at which 50 and 10 % of the soil weight are finer, respectively. The plasticity index of the silt $I_p(\%) = 5.0$, and C_u is the coefficient of uniformity. The variation in e_{max} (maximum void ratio corresponding to the loosest state of the soil sample) and e_{min} (minimum void ratio corresponding to the densest state of the soil sample) versus the fines content F_c (the ratio of the weight of silt to the total weight of the sand–silt mixture) is shown in Fig. 2. It can be clearly seen that these two indices decrease with the increase in the fines content until $F_c = 30\%$, and then, they increase with further increase in the amount of fines.

2.2 Soil Sample Preparation

The samples were prepared by means of a mould composed of two semi-cylindrical shells. The two parts of the mould can be easily joined by a hose clamp. Figure 3 shows the experimental device fabricated for the dry pluviation depositional method.

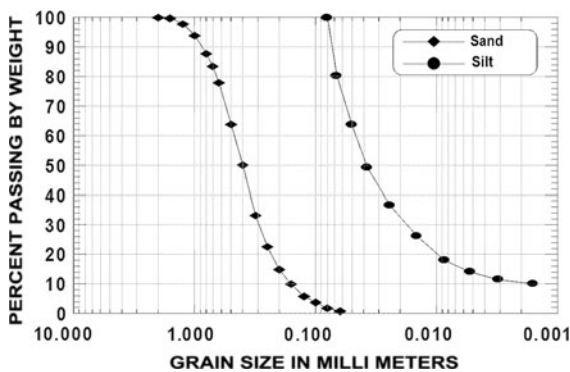


Fig. 1 Grain distribution curves of silt and sand

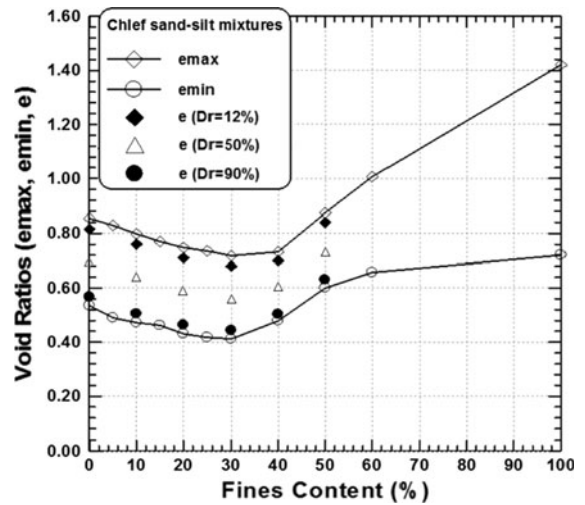


Fig. 2 Extreme and global void ratios of samples for different relative densities versus fines content

The used samples are cylindrical in shape of 70 mm in diameter and 70 mm in height ($l/d = 1.0$) (Yamamoto and Wood 2004). The mass of sand–silt mixture to be put inside the mould is computed according to the required relative density (initial volume is known), and the state of density of the sample is defined by the relative density D_r , as:

$$D_r = \frac{e_{max} - e}{e_{max} - e_{min}} 100 \% \tag{1}$$

where e is the global void ratio

2.3 Laboratory Investigation

The experimental laboratory testing was carried out on reconstituted saturated samples in order to elucidate how the fines fraction affects the undrained residual shear strength and the liquefaction potential of Chlef sand–silt mixtures. In this study, a series of undrained

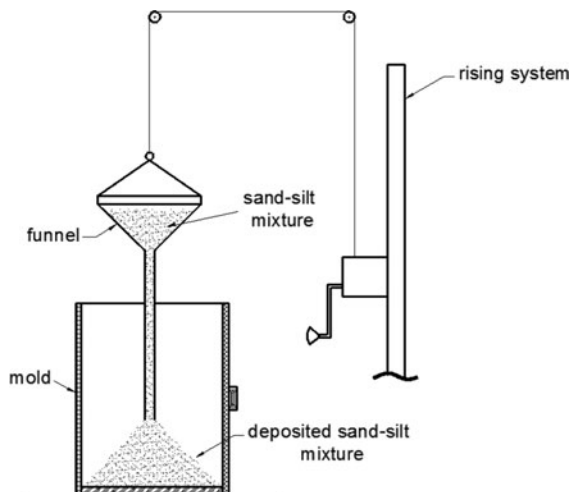


Fig. 3 Dry funnel deposition system

monotonic and cyclic triaxial tests were conducted on soil samples containing various non-plastic silt content ranging from 0 to 40 %. All specimens were prepared by estimating the dry weights of sand and silts for all relative density states under study. Samples were reconstituted using under-compaction method in order to obtain a desired proportion of the loose, medium dense and dense states ($D_r = 12, 50$ and 90 %). This preparation method produces a relatively homogeneous soil condition. This is performed by compacting dry soil in layers to the required dry unit weight of the specimen (Ladd 1978). After forming the specimen, a cap is placed on it and then sealed with O-rings. A partial vacuum of 20 kPa is applied to the sample with the aim of reducing the disturbances. In order to obtain a quasi-full saturation of the samples, the dry specimen was purged with carbon dioxide for approximately 30 min. Deaired water was then introduced into it from the bottom drain line. Water was allowed to flow through the sample, until an amount equal to the void volume of the specimen was collected in a beaker through the specimen's upper drain line. A minimum Skempton coefficient value of greater than 0.96 was obtained at back pressure of 100 kPa. All test specimens were isotropically consolidated at mean effective pressure of 100 kPa and then subjected to undrained monotonic and cyclic triaxial loading (cell pressure = 600 kPa and back pressure = 500 kPa). The used device consists of an autonomous triaxial cell, three pressure/volume controllers, and data acquisition and test control computer system, as shown in Fig. 4.



Fig. 4 Experiment device

In this study, all the undrained triaxial tests were conducted at a constant strain rate of 0.167 % per minute, which was slow enough to allow pore pressure change to equalize the sample with the pore pressure measured at the base of sample. All the tests were continued up to 24 % axial strain.

3 Tests Results

3.1 Monotonic Test Results

3.1.1 Undrained Compression Loading Tests

Standard undrained compression tests were carried out on loose, medium dense and dense samples ($D_r = 12, 50, 90$ % during reconstitution) for several fines content ranging from 0 to 40 % at 100 kPa confining pressure for three separate initial relative densities. Results of the tests are represented in Figs. 5, 6, 7, 8 and 9.

From Figs. 5, 6, 7, 8 and 9, it can be seen that large differences in behaviour between all samples are noticeable.

Generally, the increase in fines content percentages leads to a decrease in the deviatoric stress for all studied fines contents. This increase results from the role of the fines in increasing the drop in effective mean stress of the sand–silt mixture, leading to a reduction in the confining effective pressure and consequently a decrease in the peak resistance of the mixture up to 30 % of fines content; beyond that, a reverse tendency is noticed. While the deviatoric stress is still decreasing, the global void ratio is increasing as shown in Fig. 10; this change in the behavioural

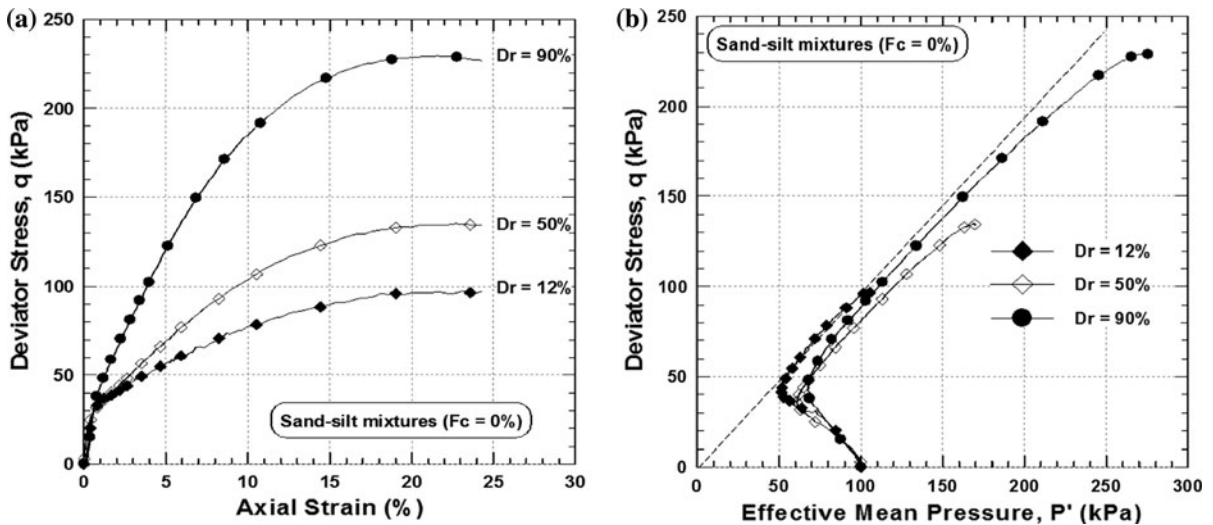


Fig. 5 **a** Test results of deviatoric stress versus axial strain (q, ϵ_a), $F_c = 0\%$. **b** Stress paths (q, p') for undrained loading tests, $F_c = 0\%$

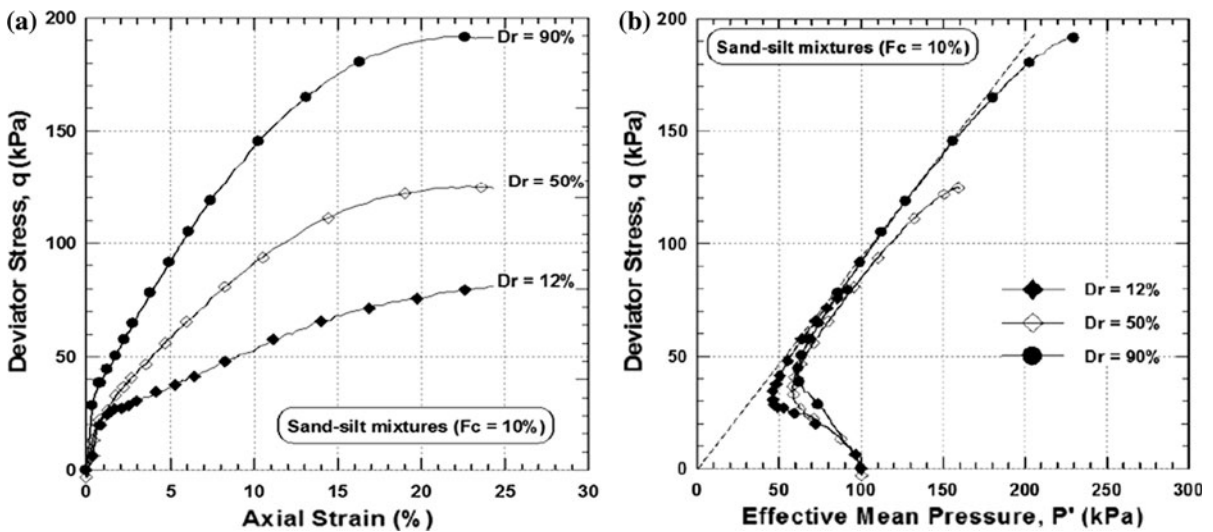


Fig. 6 **a** Test results of deviatoric stress versus axial strain (q, ϵ_a), $F_c = 10\%$. **b** Stress paths (q, p') for undrained loading tests, $F_c = 10\%$

pattern means the change in behaviour from silty sand to sandy silt, as illustrated in Figs. 5a, 6a, 7a, 8a and 9a. The stress path in the (q, p') plane shows clearly the role of the fines increase in the reduction in the average effective pressure and the maximum deviatoric stress (Figs. 5b, 6b, 7b, 8b, 9b).

In this case, the effect of fines on the undrained behaviour of the mixture is observed for the lower fines contents (0 and 10 %) and becomes very pronounced beyond 20 % until 30 %. These results

are in good agreement with the observations of Shen et al. (1977) and Troncosco and Verdugo (1985). Table 2 presents the summary of the undrained monotonic tests.

3.1.2 Normalized Undrained Residual Strength

When loose sand is subjected to undrained shearing beyond the point of peak strength, the undrained shear strength drops to a near-constant value over large

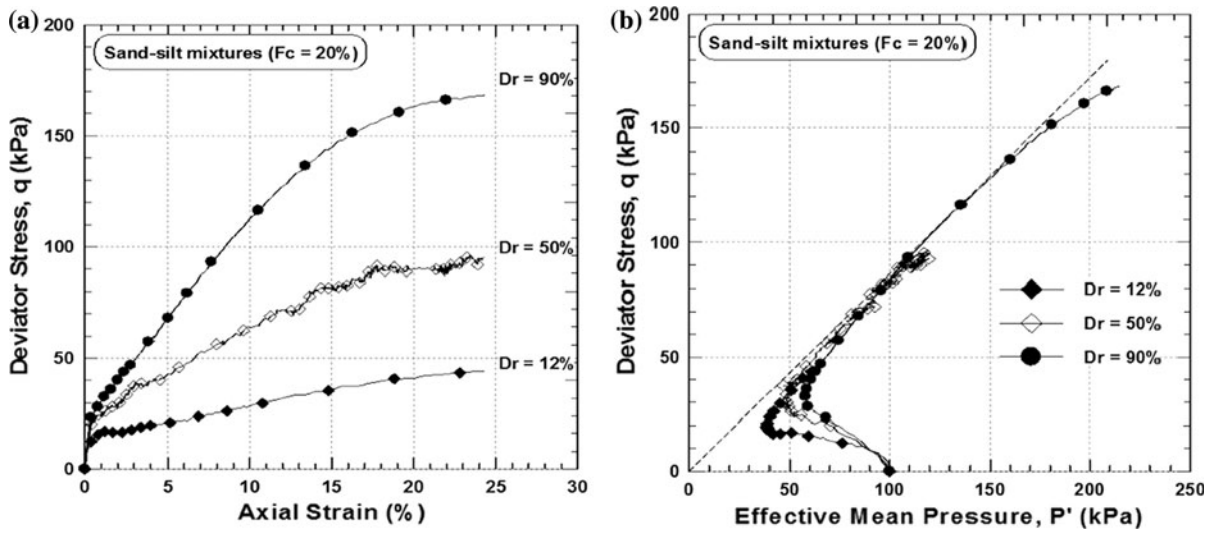


Fig. 7 a Test results of deviatoric stress versus axial strain (q, ϵ_a), $F_c = 20\%$. b Stress paths (q, p') for undrained loading tests, $F_c = 20\%$

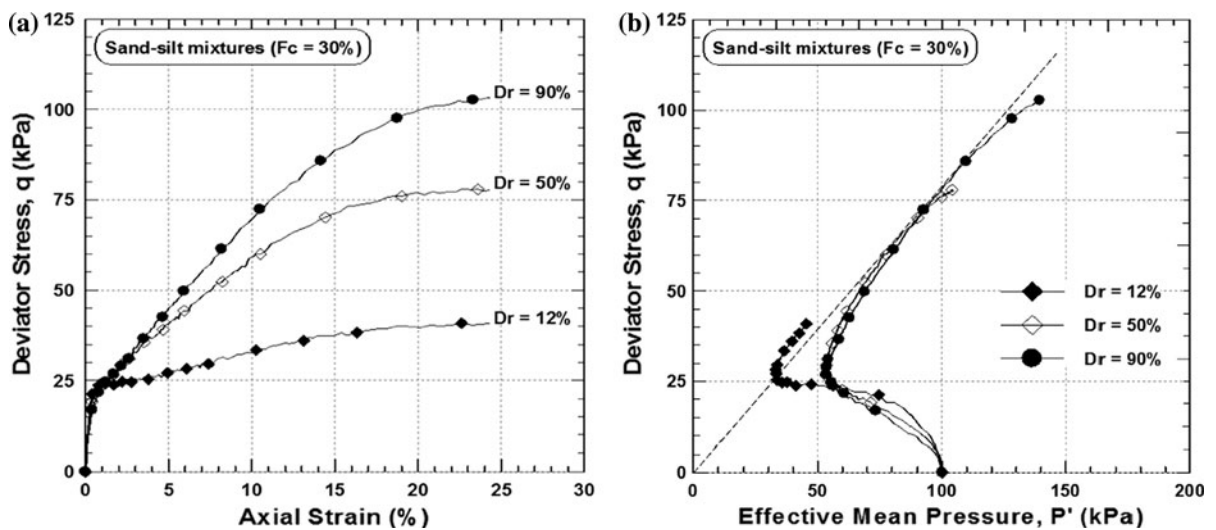


Fig. 8 a Test results of deviatoric stress versus axial strain (q, ϵ_a), $F_c = 30\%$. b Stress paths (q, p') for undrained loading tests, $F_c = 30\%$

deformation. Conventionally, this shear strength is called the undrained steady-state shear strength or residual shear strength. However, if the strength increases after passing through a minimum value, the phenomenon is called limited or quasi-liquefaction. Even limited liquefaction may result in a large deformation and associated drop in soil resistance. The residual shear strength is defined by Ishihara (1993) as

$$S_{us} = (q_s/2) \cos \phi_s = (M/2) \cos \phi_s (p'_s) \quad (2)$$

where

$$M = (6 \sin \phi_s) / (3 - \sin \phi_s) \quad (3)$$

q_s, p'_s and ϕ_s indicate the deviatoric stress ($\sigma'_1 - \sigma'_3$), the effective mean principal stress $(\sigma'_1 + 2\sigma'_3)/3$ and the mobilized angle of inter-particle friction at the

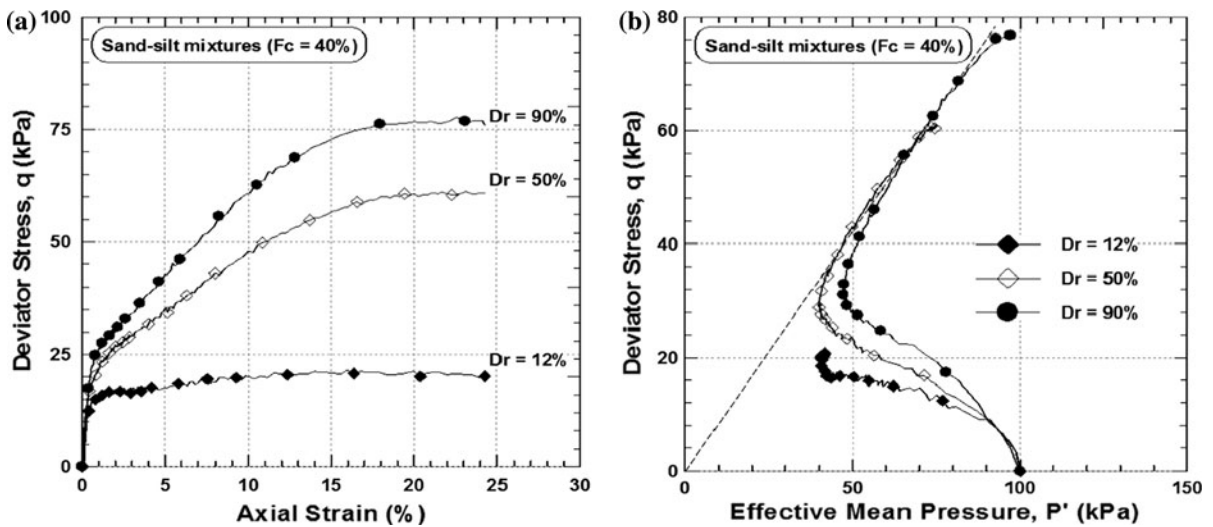


Fig. 9 a) Test results of deviatoric stress versus axial strain (q, ϵ_a), $F_c = 40\%$. b) Stress paths (q, p') for undrained loading tests, $F_c = 40\%$

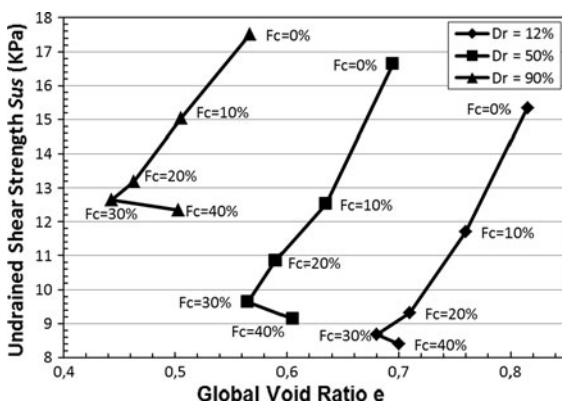


Fig. 10 Undrained residual shear strength versus global void ratio for different relative densities ($\sigma_c = 100$ kPa)

quasi-steady state (QSS), respectively. For the undrained tests conducted at the confining pressure and various initial relative densities, the deviatoric stress (q_s) was estimated at phase transition point along with the mobilized friction angle. Further, the residual shear strength can be determined by Eq. (2). The steady-state undrained shear strength results are given for different fines content fractions and for the studied relative densities in Table 2.

The residual shear strength (S_{us}) changes with the initial relative density ($D_r = 12, 50$ and 90%

measured during reconstitution) at various fines contents are shown in Fig. 11. It is clear from Fig. 11 that an increase in the relative density results in an increase in the residual shear strength at a given fines content. The present laboratory study focuses on the effect of equivalent void ratio on the residual shear strength of sand–silt mixtures at various initial relative densities ($D_r = 12, 50$ and 90% during reconstitution). It can be noticed from the results of this investigation that there is a significant increase in the residual shear strength with increase in the initial relative density and a significant decrease in the residual strength with the increase in the fines content. The trend of the present results is similar to the experimental work reported by Ishihara (1993) on Tia Juana silty sand and by Naeini and Baziar (2004) on Adebil sand mixed with different amounts of fines.

Thus, the initial relative density is a major governing parameter for susceptibility to liquefaction phenomenon. Meanwhile, the fines content is a variable in the equivalent void expression. The undrained steady shear strength can be better represented by the initial relative density as shown in Fig. 11. It is clear that the steady state shear strength can be correlated with the initial relative density in a linear form.

The obtained expressions for different fines contents are given as follows:

Table 2 Undrained monotonic test results for different relative densities of sand–silt mixtures

Materials	Test no.	F_c Fines content (%)	D_r Initial relative density (%)	γ_d Soil dry density (kN/m ³)	e Global void ratio	S_{us} Residual undrained shear strength (kPa)
Clean sand	1	0	12	14.8	0.815	15.33
	2		50	15.8	0.695	16.63
	3		90	17.1	0.567	17.51
Silty sand	4	10	12	15.2	0.760	11.70
	5		50	16.4	0.635	12.53
	6		90	17.8	0.505	15.04
	7	20	12	15.7	0.710	9.31
	8		50	16.9	0.590	10.86
	9		90	18.3	0.463	13.18
	10	30	12	16.0	0.680	8.67
	11		50	17.1	0.565	9.64
	12		90	18.6	0.443	12.65
	13	40	12	15.8	0.700	8.40
	14		50	16.7	0.605	9.13
	15		90	17.9	0.503	12.35

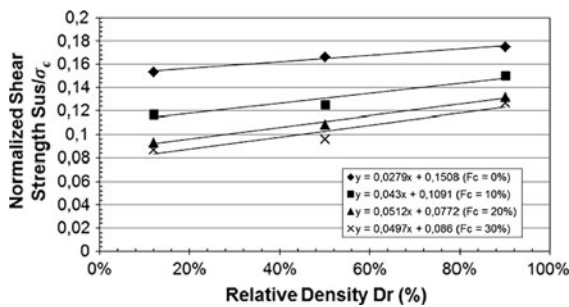


Fig. 11 Correlations between normalized residual shear strength and relative density for different fines content

$$\begin{aligned}
 S_{us}/\sigma_c &= 0.1508 + 0.0279D_r \quad \text{for } F_c = 0\% \\
 S_{us}/\sigma_c &= 0.1091 + 0.0430D_r \quad \text{for } F_c = 10\% \\
 S_{us}/\sigma_c &= 0.0772 + 0.0512D_r \quad \text{for } F_c = 20\% \\
 S_{us}/\sigma_c &= 0.086 + 0.0497D_r \quad \text{for } F_c = 30\%
 \end{aligned}
 \tag{4}$$

From this study, for each fines content, the same behavioural pattern can be seen from Fig. 11 of silt–sand mixture with different initial relative densities.

It is obvious from Fig. 11 that the undrained residual shear strength increases with the increase in the initial relative density for all fines content up to 30%. Also, the undrained steady shear strength decreases with the increase in fines content.

3.2 Equivalent Void Ratio

When the behaviour of sand–silt mixtures is controlled by the force chain in sand particles, the silt is simply supposed to be occupying void in the sand skeleton; this assumption has led to the introduction of the concept of inter-granular void ratio, expressed in the following form,

$$e_s = (e + (F_c/100))/(1 - (F_c/100)) \tag{5}$$

where e is the global void ratio and F_c is the fines content. Equation (1) gives the inter-granular void ratio defined by Thevanayagam (1998). The concept of the inter-granular void ratio suggests that the fines fill the voids formed between the sand grains and thus the behaviour of sand with moderate amount of fines should be governed by the inter-granular void ratio instead of the global void ratio. However, when the inter-granular void ratio exceeds the maximum void ratio of the clean sand, there are sufficient fines to prevent grain-to-grain contact of the sand particles. In this case, the fines constitute the dominant structure and carry the shear forces while the coarse grains may act as reinforcing elements (Thevanayagam and Mohan 2000).

Zlatovic and Ishihara (1995) and Pitman et al. (1994) reported that fines particle started to come in between sand particle contacts at 5% fines content

and sand particle contacts vanished completely at 30 % silt content. Based on that, an equivalent void ratio mathematical expression (6) was formulated in order to satisfy these experimental observations (Thevanayagam et al. 2002). A general form of the equivalent void ratio can be written as:

$$e^* = (e + \alpha \cdot F_c)/(1 - \alpha \cdot F_c) \tag{6}$$

where α is the fraction of fines which do not participate in the force structure of the solid skeleton; when $\alpha = 1$, equivalent granular void ratio is reduced to inter-granular void ratio. Generally, e^* is obtained from correlation between soil grading properties and back-analysed values (Ni et al. 2004; Yang et al. 2006). Recently, Rahman et al. (2008) analysed the experimental data of Mc Geary (1961) on binary packing studies and concluded that α should be dependent on both particles size ratio (r) and fines content (F_c). The size ratio r is defined by $r = (D_{50(\text{fine})}/D_{10(\text{sand})})$ where $D_{50(\text{fine})}$ is the median size of fines and $D_{10(\text{sand})}$ is the particle size at 10 % fractile for host sand. Correlation was suggested in the present form:

$$\alpha = 1 - \{[1 - \exp[-0.3(F_c/F_{\text{thre}})/k]](rF_{\text{thre}}/F_c)^r\} \tag{7}$$

where $k = 1 - r^{0.25}$, F_{thre} is threshold fines content or transitional fines content, which is characterized by the predominance of fines behaviour. Thus, the value of F_{thre} is defined by the point where the behaviour trend reverses with further increase in fines content. From our tests, this transition point is located at 30 % fines content for all three initial relative densities as shown in Fig. 8. For Chlef sand–silt mixture, r and k were calculated to be: $r = 0.361$ and $k = 0.225$.

The variation in the global and equivalent void ratios versus fines content for the initial relative densities ($D_r = 12, 50$ and 90%) is shown in Fig. 12. For all studied initial relative densities, it can be seen that a decrease in the global void ratio generates an increase in the equivalent void ratio. The absolute rate of variation in both void ratios tends to decrease as long as the fines contents increases.

Figure 13 shows the residual shear strength variation versus the equivalent void ratio. It is obvious from this that the undrained shear strength decreases linearly as the equivalent void ratio decreases and fines content increases for all densities ($D_r = 12, 50$ and 90% during reconstitution) up to 30 % fines content. It means that when decreasing the global void

ratio and increasing the fines content, the undrained residual shear strength also decreases. It can be concluded that the global void ratio does not represent the real behaviour of silty sand soil with 0–30 % fines content. Moreover, the equivalent void ratio is a key parameter for characterizing the mechanical state of clean sand as well as sand–silt mixtures.

The following correlation is obtained for all ranges of relative density under study:

$$S_{us}/\sigma_c = 0.2734 - 0.1866 e^* \tag{8}$$

3.3 Cyclic Tests Results

3.3.1 Compression–Extension Tests

During an earthquake shaking, the pore water pressure in a saturated sandy soil will increase due to the

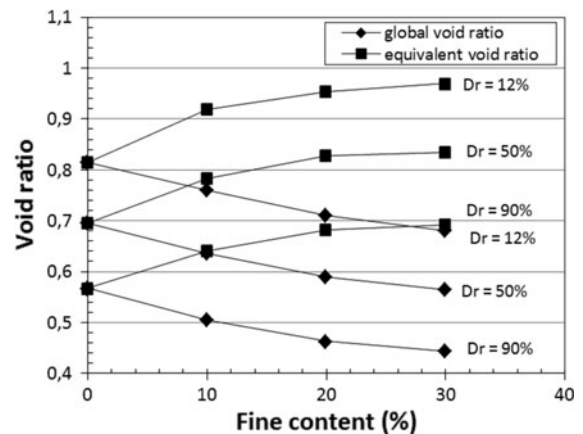


Fig. 12 Global and equivalent void ratios for different relative densities of sand–silt mixtures

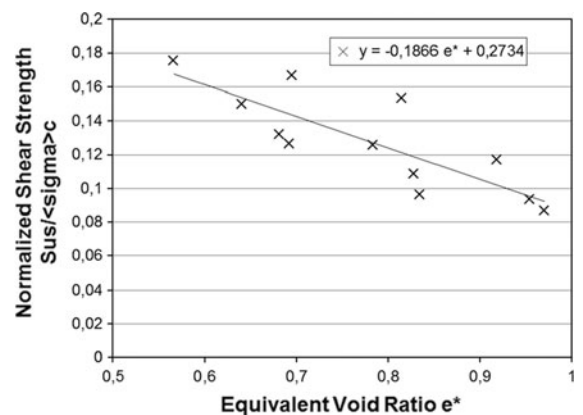


Fig. 13 Curves fitting for normalized residual shear strength and equivalent void ratio for different relative densities

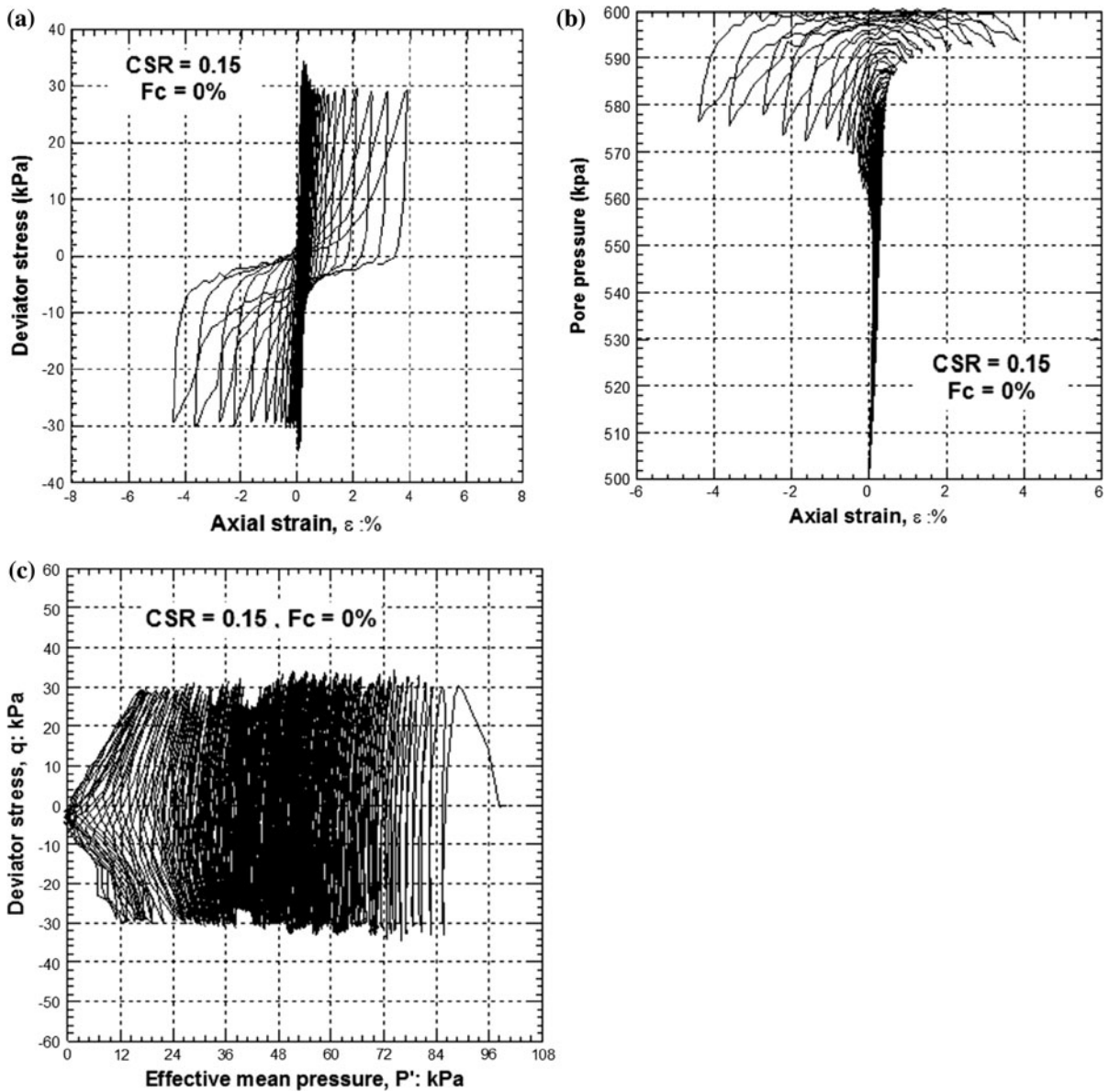


Fig. 14 Cyclic test on clean sand ($e = 0.695$, $e^* = 0.695$, $D_r = 50\%$, $CSR = 0.15$, $\sigma_c = 100$ kPa)

tendency of the volume contraction if the drainage of water is impeded. Due to this fact, undrained conditions reasonably simulate earthquake loading.

Evaluation of the liquefaction potential is accomplished by comparing equivalent measures of earthquake loading and liquefaction resistance. The most common approach to characterize earthquake loading is the use of cyclic shear stresses. By normalizing the cyclic shear stress amplitude by the initial effective vertical stress, a cyclic stress ratio (CSR) can represent

the level of loading induced at different depths in a soil profile by an earthquake. A simplified approach may be used to estimate CSR as a function of peak ground surface acceleration amplitude (Seed and Idriss 1981).

In this context, the effect of different deviatoric stress amplitude levels along with varying fines content on the liquefaction potential is analysed.

Soil samples were prepared by varying silt content from 0 to 30 % with an initial relative density of 50 %. Three series of stress-controlled cyclic triaxial tests

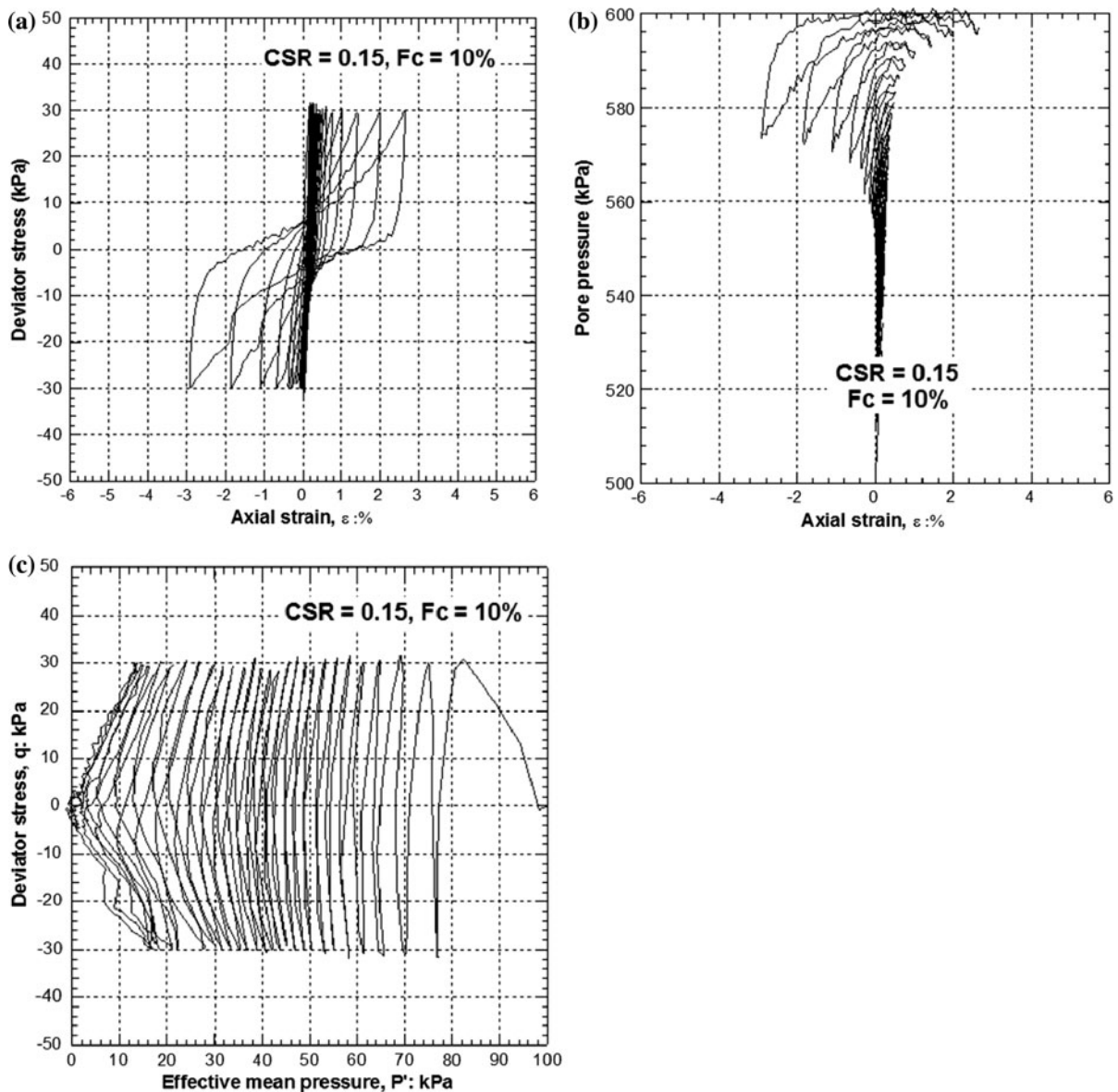


Fig. 15 Cyclic test on silty sand ($e^* = 0.738$, $D_r = 50\%$, $CSR = 0.15$, $\sigma_c = 100$ kPa)

were performed on isotropically consolidated silty sand mixture specimens, and alternated symmetric deviatoric stress was applied under undrained conditions to simulate essentially undrained field conditions during earthquakes. Since the predominant frequency in an earthquake generally lies between 0.2 and 1.0 Hz. All experiments were conducted for three different accelerations at a constant frequency of 0.5 Hz. The class level of accelerations covers the nature of moderate and strong earthquakes

($M = 5.0 - 8.0$). In the first one, three alternated cyclic tests were conducted on clean sand samples ($e = e^* = 0.695$) with a relative density of 50% and a confining initial pressure of 100 kPa. The cycles amplitudes (q_m) used were 30, 50 and 70 kPa, respectively. The second test was established on the mixture silt–sand samples with a global void ratio of 0.635 and 10% of fines content corresponding to $e^* = 0.783$, and loading amplitudes of 30, 40 and 60 kPa; while in the third series of tests, experiments

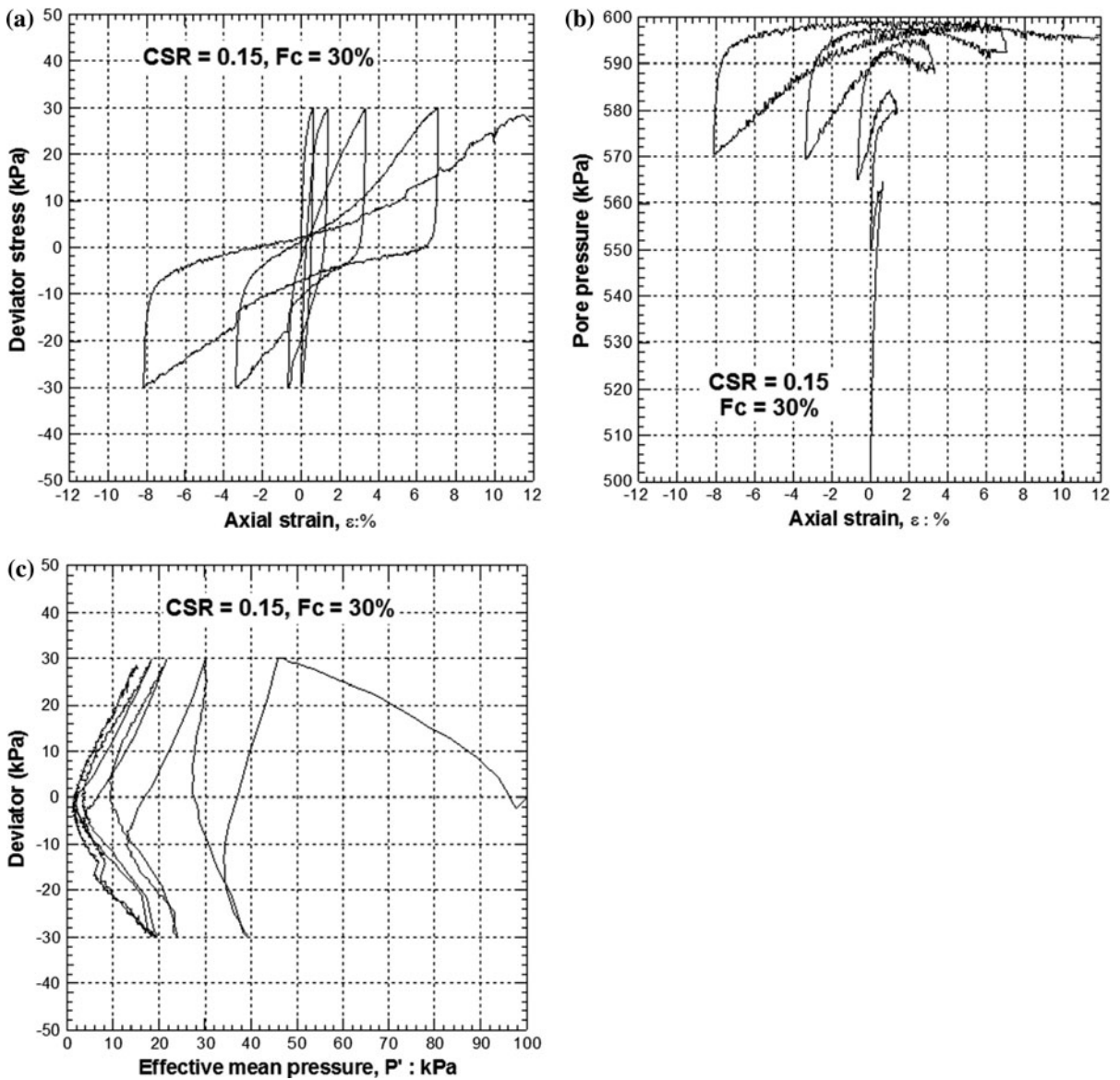


Fig. 16 Cyclic test on silty sand ($e^* = 0.835$, $D_r = 50\%$, $CSR = 0.15$, $\sigma_c = 100$ kPa)

were conducted on samples with an equivalent void ratio of 0.835 with 30 % fines content and by applying loading amplitudes of 20, 30 and 50 kPa. In all tests, the pore pressures were generated in each loading cycle resulting in an accumulation of excess pore pressure, and large deformation continued to develop, resulting in moving the effective stress path to failure, which coincides with formation of large wrinkles visible in the membrane surrounding the specimen. It has been noted that the fines contents affect considerably the liquefaction of the samples. Figure 14

illustrates the results of the test carried out on clean sand samples ($e = e^* = 0.695$) with loading amplitude of 30 kPa.

It is clear from Fig. 14 that as the number of cycles increases, the pore water pressure increases for all silt contents which automatically leads to a reduction in the average effective pressure. The rate and magnitude of pore pressure generation during cyclic loading have a major effect on the strength of the soil stability and consequently on structures founded on it. The rate of increase in the pore pressure remains low, because

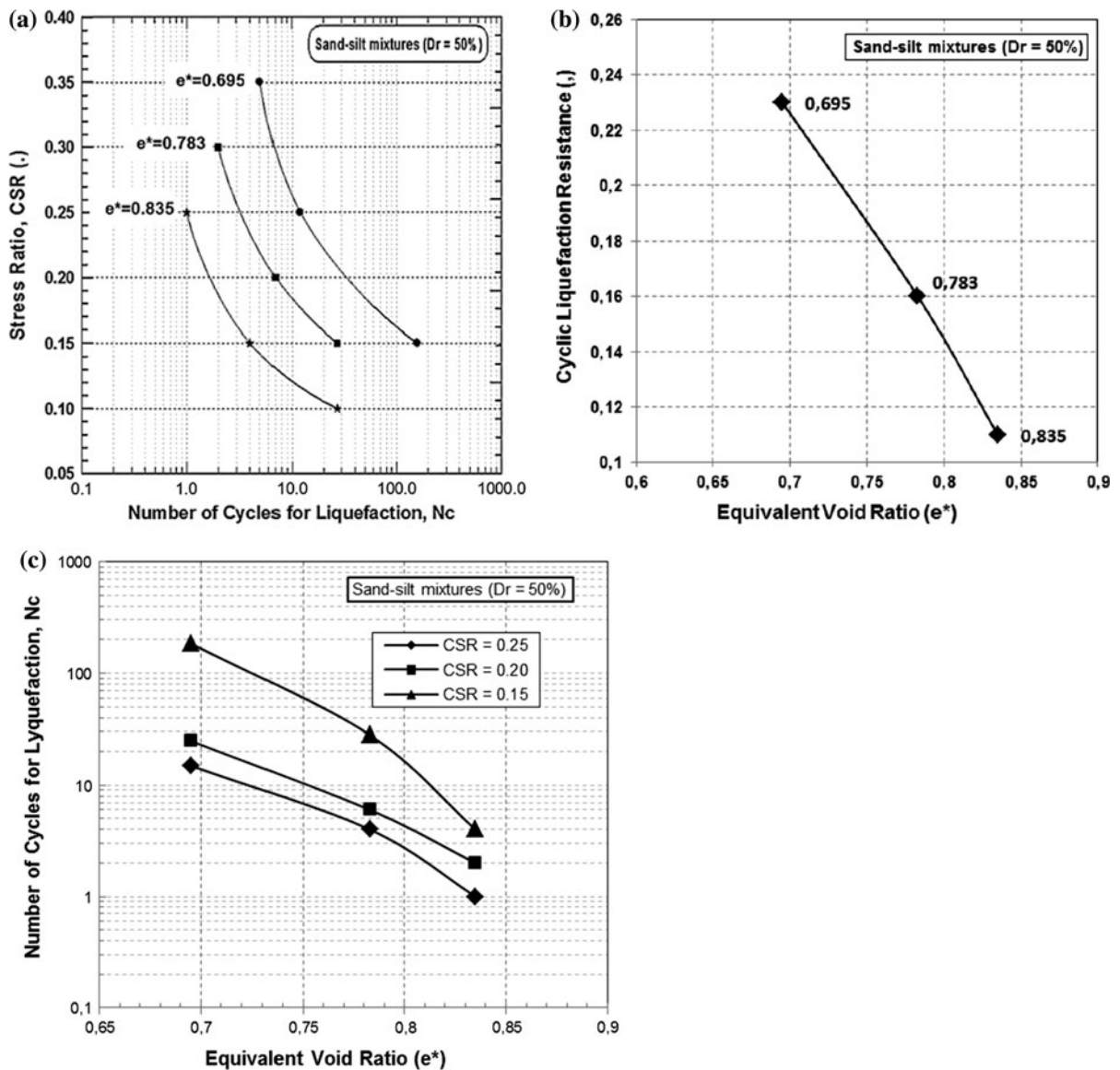


Fig. 17 Effect of the equivalent void ratio on the liquefaction potential of the sand–silt mixtures ($\sigma_c = 100$ kPa, $D_r = 50\%$)

liquefaction is obtained only after 158 cycles; for the test with $q_m = 30$ kPa and a global void ratio of 0.635 and 10 % of fines content corresponding to $e^* = 0.783$ (Fig. 15), we notice a significant increase in the pore water pressure during 27th cycle with a significant axial strain (2.5 %) leading to the liquefaction of the sample.

For the test with a loading amplitude of 30 kPa and a global void ratio of 0.565 and 30 % fines content corresponding to $e^* = 0.835$, we notice a significant increase in the pore water pressure during the 3rd cycle with an axial strain leading to the liquefaction of the

sample to the 4th cycle (Fig. 16). It can be concluded that the increase in fines content in the range of (0–30 %) promotes the risk of liquefaction. These observations are in a good agreement with the results reported by Finn et al. (1994).

3.3.2 Influence of the Equivalent Void Ratio on the Potential of Liquefaction

The variation in the cyclic stress ratio ($CSR = q_{max}/2\sigma'_c$) with respect to the number of cycles leading to liquefaction (N_c) for $D_r = 50\%$ is shown in Fig. 17a.

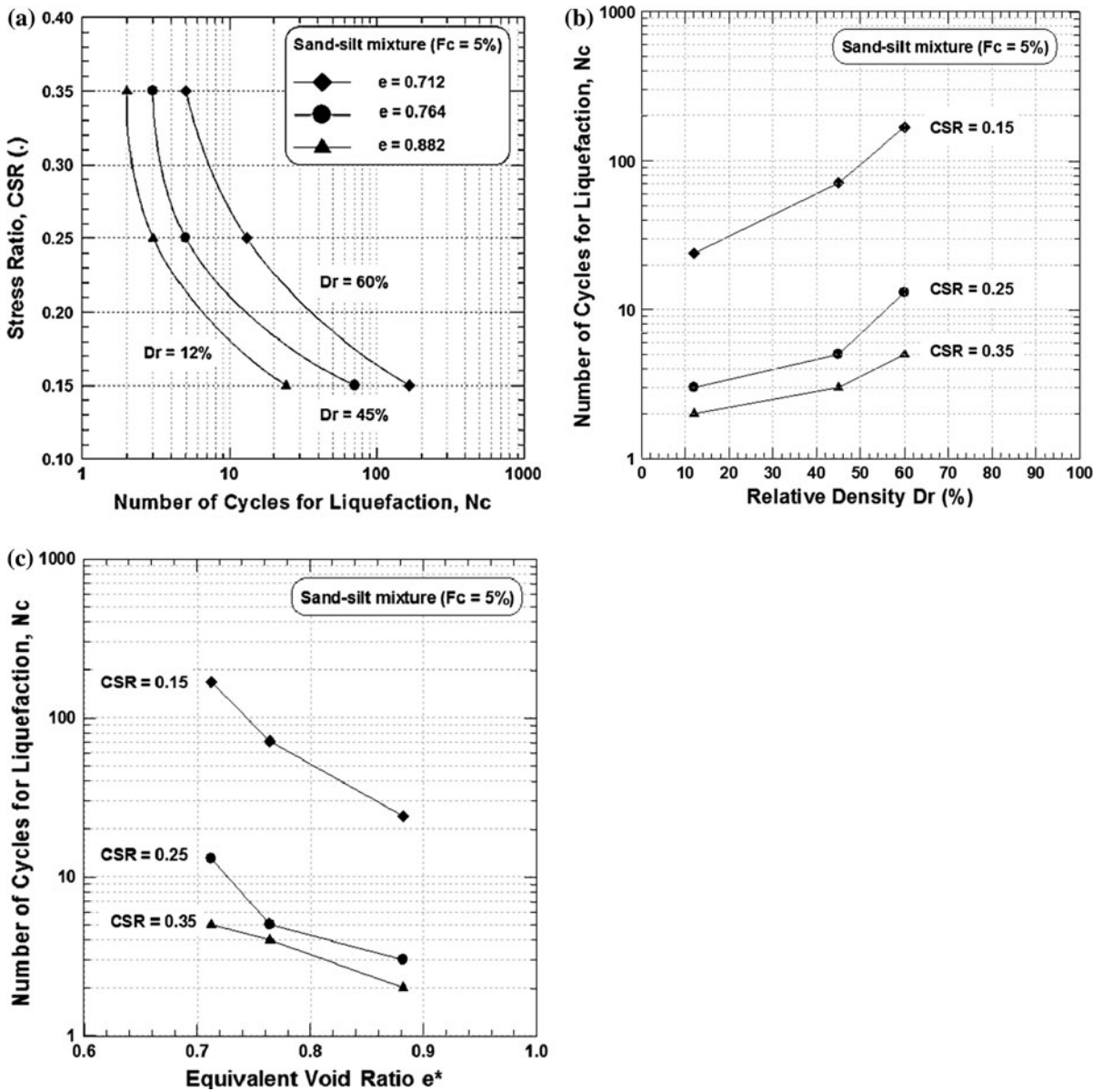


Fig. 18 Effect of the initial relative density on the liquefaction resistance of the sand-silt mixture ($\sigma_c = 100$ kPa, $F_c = 5\%$)

It is clear that when the cyclic stress increases, the number of cycles for liquefaction (N_c) decreases for all studied equivalent void ratios e^* . The same behavioural trend is obtained for all conducted tests.

Figure 17b illustrates linear variation for cyclic liquefaction resistance in terms of the equivalent void ratio e^* . Also, the cyclic liquefaction resistance (CLR) decreases with the increase in the equivalent void ratio for the studied density. The change in the number of cycles (N_c) leading to liquefaction with respect to the

void ratio for all studied cyclic ratios is represented in Fig. 17c.

Cyclic liquefaction resistance (CLR) is defined as the cyclic stress ratio causing the liquefaction at 15 cycles, according to Ishihara (1993). It can be deduced that liquefaction potential of the sand-silt mixtures decreases with the increase in the fines content. These results are in good agreement with those found in monotonic tests showing that the increase in fines content amplifies the drop in effective mean stress.

Consequently, the decrease in effective mean stress induces a reduction in the liquefaction potential when the fines content increases. It should be noted that for the studied amplitude ($q_m = 30$ kPa), the increase in the range of 0–30 % fines content induces an acceleration of liquefaction phenomenon. We notice that the liquefaction resistance decreases with the increase in the fines content. The samples sheared under higher loading level ($CSR = 0.25$) are more vulnerable to liquefaction than those sheared with smaller loading level ($CSR = 0.15$).

3.3.3 Effect of the Relative Density

In order to study the influence of the relative density on liquefaction phenomenon, undrained cyclic tests were carried out on Chlef sand–silt mixture ($F_c = 5$ %) for three initial relative densities ($D_r = 12, 45$ and 60 % during reconstitution). The loading amplitude has been varied for each density, in order to depict the liquefaction potential curve. The used amplitudes are $q_m = 30, 50$ and 70 kPa. It can be noted that the liquefaction is reached quickly for the higher amplitudes after two and three cycles, respectively, for the loading amplitudes of $q_m = 70$ and 50 kPa, whereas the liquefaction under the loading amplitude $q_m = 30$ kPa for the tests carried out with a relative density $D_r = 12$ % (measured during reconstitution) is reached at 24 cycles; for the same loading amplitudes, the liquefaction is obtained only after 3, 5 and 71 cycles for the tests with a relative density $D_r = 45$ % (measured during reconstitution). For the tests carried out with a relative density $D_r = 60$ % (measured during reconstitution) and for the same loading amplitudes, the liquefaction is reached at 5, 13 and 167 cycles. The results of these tests are summarized in Fig. 18.

The influence of the relative density (measured during reconstitution) on the liquefaction potential of sand–silt mixture ($F_c = 5$ %) is represented in Fig. 18a, b. It can be seen clearly that the increase in the initial relative density leads to an increase in the liquefaction resistance of the sand–silt mixture, while Fig. 18c shows the influence of the equivalent void ratio on the liquefaction resistance defined by the amplitude of the loading inducing liquefaction after 15 cycles for the Chlef sand–silt mixture. Figure 18c shows clearly that the increase in the equivalent void ratio and the loading amplitude decreases the

liquefaction resistance. It should be added that the reduction in the liquefaction resistance of sand–silt mixture becomes very pronounced for the smaller cyclic stress ratios $CSR = 0.15$ and 0.25 .

4 Conclusion

This laboratory investigation has been conducted on Chlef sand–silt mixtures in order to evaluate the undrained steady-state shear strength and the liquefaction potential under the effect of the amount of fine hosted by the sand and for different initial relative density states. From these experiments, it can be noticed that the participation of fines fraction in force chain of the soil may be strongly interpreted by means of the equivalent void ratio. This property may be introduced as a state parameter in order to characterize the dilatancy behaviour of silty sands vulnerable to liquefaction phenomenon.

Moreover, the following conclusions can be drawn:

Undrained monotonic triaxial tests on loose, medium dense and dense silty sand indicate clearly that there is a correlation between the undrained residual shear strength (S_{us}) and the equivalent void ratio e^* provided that the fines content should be less or equal to 30 %, since the concept of the equivalent void ratio is valid till 30 % of fines content in our case due to the reverse tendency of the undrained residual shear strength observed beyond $F_c = 30$ %. It is shown that for the range 0–30 % of the fines content, the undrained residual shear strength decreases linearly with increase in equivalent void ratio. As well, the undrained residual shear strength increases linearly with the increase in the initial relative density for all fines contents. A unique relationship has been deduced for the change in the residual shear strength with respect to the equivalent void ratio for all the range of the relative densities.

Undrained cyclic test results show that liquefaction potential of the sand–silt mixtures decreases with increase in the equivalent void ratio (fines content) and the samples sheared with higher level loading ($CSR = 0.25$) are more vulnerable to liquefaction than those sheared with smaller loading level ($CSR = 0.15$). They also show that the liquefaction resistance increases with the relative density, but it decreases with the increase in the equivalent void ratio and the loading amplitude. We note that the reduction in the liquefaction resistance of Chlef sand–silt mixture becomes very pronounced for the

smaller cyclic stress ratios $CSR = 0.15$ and 0.25 . Also, the pore water pressure development during any harmonic loading can be regarded in terms of the number of cycles of loading that the soil has undergone.

From both monotonic and cyclic tests results, it can be seen that the increase in the equivalent void ratios amplifies the effective mean stress decrease range. Consequently, this behaviour leads to a reduction in the liquefaction potential. These observations are valid for all studied tests. It should be noted that for the loading amplitude ($q_m = 30$ kPa), the increase in the equivalent void ratio in the range of 0–30 % fines content accelerates the liquefaction phenomenon of the studied sand–silt mixtures. The cyclic resistance of the soil can be controlled by the relative density of soil sample as well as by the fines contents.

References

- Bouferra R, Shahrouf I (2004) Influence of fines on the resistance to liquefaction of a clayey sand. *Ground Improv* 8(1):1–5
- Carraro JAH, Bandini P, Salgado R (2003) Liquefaction resistance of clean and nonplastic silty sands based on cone penetration resistance. *J Geotech Geoenviron Eng ASCE* 129(11):965–976
- Chang NY, Yeh ST, Kaufman LP (1982) Liquefaction potential of clean and silty sands. In: *Proceedings of 3rd international microzonation conference, vol 2*. Seattle, USA, pp 1017–1032
- Della N, Arab A, Belkhatir M, Missoum H (2009) Identification of the behaviour of the Chlef sand to static liquefaction. *Comptes Rendus de Mécanique* 337(5):282–290
- Dobry R, Ladd RS, Yokel FY, Chung RM, Powell D (1982) Prediction of pore pressure build up and liquefaction of sands during earthquake by cyclic strain method. National Bureau of Standards, N.B.S. Building Science Series, Washington, DC 138
- Finn WDL (2000) State-of-the-art of geotechnical earthquake engineering practice. *Soil Dyn Earthq Eng* 20:1–15
- Finn WDL, Ledbetter RH, Wu G (1994) Liquefaction in silty soils: design and analysis. Ground failures under seismic conditions. *Geotech Special Publ ASCE* 44:51–76
- Georginno VN, Burland JB, Hight DW (1990) The undrained behaviour of clayey sands in triaxial compression and extension. *Géotechnique* 40(3):431–449
- Idriss IM, Boulanger RW (2008) *Soil liquefaction during earthquakes*. Earthquake Engineering Research Institute, Oakland, CA
- Ishihara K (1993) Liquefaction and flow failure during earthquakes. *Géotechnique* 43(3):351–415
- Kenny TC (1977) Residual strengths of mineral mixtures. *Proceedings of the 9th international conference on soil mechanics foundation engineering, Tokyo, vol 1*, pp 155–160
- Kishida H (1969) Characteristics of liquefied sands during Mino-Owari, Tohankai and Fukui earthquakes. *Soils Found* 9(1):75–92
- Koester JP (1994) Liquefaction characteristics of silt. *Ground failures under seismic condition. Geotech Special Publ ASCE* 44:105–116
- Ladd RS (1978) Preparing test specimen using under compaction. *Geotech Test J GTJODJ* 1:16–23
- Lade PV, Yamamuro JA (1997) Effects of non-plastic fines on static liquefaction of sands. *Can Geotech J* 34:918–928
- Law KT, Ling YH (1992) Liquefaction of granular soils with non-cohesive and cohesive fines. In: *Proceedings of the 10th world conference on earthquake engineering, Rotterdam*, pp 1491–1496
- Maheshwari BK, Patel AK (2010) Effects of non-plastic silts on liquefaction potential of Solani sand. *Geotech Geol Eng* 28:559–566
- Mc Geary RK (1961) Mechanical packing of spherical particles. *J Am Ceram Soc* 44(10):513–522
- Mitchell JK (1993) *Fundamentals of soil behaviour*, 2nd edn. John Wiley Inter-science, New York
- Naeini SA, Baziar MH (2004) Effect of fines content on steady-state strength of mixed and layered samples of a sand. *Soil Dyn Earthq Eng* 24(3):181–187
- Ni Q, Tan TS, Dasari GR, Hight DW (2004) Contribution of fines to the compressive strength of mixed soils. *Géotechnique* 54(9):561–569
- Pitman TD, Robertson PK, Sego DC (1994) Influence of fines on the collapse of loose sands. *Can Geotech J* 31(5):728–739
- Rahman MM, Lo SR, Gnanendran CT (2008) On equivalent granular void ratio and steady state behaviour of loose sand with fines. *Can Geotech J* 45(10):1439–1455
- Seed HB, Idriss IM (1981) Evaluation of liquefaction potential of sand deposits based on observations and performance in previous earthquakes. Pre-print No. 81–544, *In Situ Testing to Evaluate Liquefaction Susceptibility, ASCE Annual Convention, St. Louis*
- Seed HB, Idriss IM, Arango I (1983) Evaluation of liquefaction potential using field performance data. *J Geotech Eng Div ASCE* 109(3):458–482
- Shen CK, Vrymoed JL, Uyeno CK (1977) The effects of fines on liquefaction of sands. In: *Proceedings of 9th international conference on soil mechanics and foundation engineering, Tokyo, vol 2*, pp 381–385
- Singh S (1994) The influence of fine type and content on cyclic strength. Ground failures under seismic condition. *Geotech Special Publ ASCE* 44:17–33
- Thevanayagam S (1997) Dielectric dispersion of porous media as a fractal phenomenon. *J Appl Phys* 82(5):2538–2547
- Thevanayagam S (1998) Effect of fines and confining stress on undrained shear strength of silty sands. *J Geotech Geoenviron Eng Div ASCE* 124(6):479–491
- Thevanayagam S, Mohan S (2000) Inter-granular state variables and stress-strain behaviour of silty sands. *Géotechnique* 50(1):1–23
- Thevanayagam S, Nesarajah S (1998) Fractal model for flow through saturated soil. *J Geotech Geoenviron Eng ASCE* 124(1):53–66
- Thevanayagam S, Shenthnan T, Mohan S, Liang J (2002) Undrained fragility of clean sands, silty sands, and sandy silts. *J Geotech Geoenviron Eng ASCE* 128(10):849–859

- Troncosco JH, Verdugo R (1985). Silt content and dynamic behaviour of tailing sands. In: Proceedings of the 12th international conference on soil mechanics and foundation engineering, San Francisco, pp 1311–1314
- Vaid YP, Sivathayalan S, Stedman D (1999) Influence of specimen reconstituting method on the undrained response of sand. *Geotech Test J* 22(3):187–195
- Yamamoto JA, Kelly MC (2001) Monotonic and cyclic liquefaction of very loose sands with high silt content. *J Geotech Geoenviron Eng ASCE* 127(4):314–324
- Yamamoto JA, Lade PV (1998) Steady-state concepts and static liquefaction of silty sands. *J Geotech Geoenviron Eng ASCE* 124(9):868–877
- Yamamoto JA, Wood FM (2004) Effect of depositional method on the undrained behaviour and microstructure of sand with silt. *Soil Dyn Earthq Eng* 24:751–760
- Yang SL, Lacasse S, Sandven RF (2006) Determination of the transitional fines content of mixtures of sand and non-plastic fines. *Geotech Test J* 29(2):102–107
- Zlatovic S, Ishihara K (1995) On the influence of non-plastic fines on residual strength. In: Proceedings of the first international conference on earthquake geotechnical engineering, Tokyo, 14–16 November, pp 239–244
- Zlatovic S, Ishihara K (1997) Normalized behaviour of very loose non plastic soils: effects of fabric. *Soils Found* 37(4):47–56